

Frontal sinuses and head-butting in goats: a finite element analysis

Andrew A. Farke

Department of Anatomical Sciences, Stony Brook University, NY 11794-8081, USA

Present address: Raymond M. Alf Museum of Paleontology, Claremont, CA 91711-2199, USA (e-mail: afarke@webb.org)

Accepted 21 July 2008

SUMMARY

Frontal sinuses in goats and other mammals have been hypothesized to function as shock absorbers, protecting the brain from blows during intraspecific combat. Furthermore, sinuses are thought to form through removal of 'structurally unnecessary' bone. These hypotheses were tested using finite element modeling. Three-dimensional models of domesticated goat (*Capra hircus*) skulls were constructed, with variable frontal bone and frontal sinus morphology, and loaded to simulate various head-butting behaviors. In general, models with sinuses experienced higher strain energy values (a proxy for shock absorption) than did models with unvaulted frontal bones, and the latter often had higher magnitudes than models with solid vaulted frontal bones. Furthermore, vaulted frontal bones did not reduce magnitudes of principal strain on the surface of the endocranial cavity relative to models with unvaulted frontal bones under most loading conditions. Thus, these results were only partially consistent with sinuses, or the bone that walls the sinuses, acting as shock absorbers. It is hypothesized that the keratinous horn sheaths and cranial sutures are probably more important for absorbing blows to the head. Models with sinuses did exhibit a more 'efficient' distribution of stresses, as visualized by histograms in which models with solid frontal bones had numerous unloaded elements. This is consistent with the hypothesis that sinuses result at least in part from the removal of mechanically unnecessary bone.

Supplementary material available online at <http://jeb.biologists.org/cgi/content/full/211/19/3085/DC1>

Key words: Bovidae, *Capra hircus*, finite element analysis, goats, head-butting, paranasal sinus, pneumaticity.

INTRODUCTION

Head-to-head combat by sheep and goats is a spectacular event, both visually and mechanically. Rival males rear back and bang their horns together, and this event may be repeated several times in succession (e.g. Alvarez, 1990). In bighorn sheep (*Ovis canadensis*) the impact force may exceed 3400 N, and the sudden deceleration of impact occurs over less than 300 ms (Kitchener, 1988). These intense impacts so near critical cranial organs [associated with coup/contrecoup injuries to the brain in humans, among other effects (e.g. Gurdjian, 1975)] have invited numerous lines of speculation on the structures that may be responsible for 'shock absorption' during combat (e.g. Geist, 1966; Jaslow and Biewener, 1995; McDonald, 1981).

Shock absorbers dampen sudden accelerations by converting applied kinetic energy into another form (e.g. heat), through deformation over a period of time. These principles have been used to develop football helmets and other protective devices, which protect the human skull and brain by attenuating impact energy through deformation of the helmet in place of the head and reducing the force directly transmitted into the skull itself and/or spreading the force over a larger area (Levy et al., 2004). Similarly, an idealized biological shock absorber in the skull experiences elastic deformation (as opposed to brittle fracture or plastic deformation) and concentrates this deformation away from delicate cranial organs. A longer period of deformation, related to the elasticity of the deforming object, reduces strains (and hence potential damage) on brain tissue and blood vessels due to inertia. Several structures within a sheep or goat skull could contribute to shock absorption. For example, the keratin sheath of the horns is considerably more elastic than bone, allowing a relatively greater amount of deformation (Kitchener, 1987; Kitchener, 1988), and the position of the sheaths localizes this deformation away from the immediate area of the brain and other cranial organs. Several cranial sutures

that are located near the horns (hence, near the area of impact), exhibit high strains during impact loads (Jaslow and Biewener, 1995), and thus may also function as a sort of 'crumple zone' during impacts. Finally, the frontal sinus system is another candidate for shock absorbers.

The frontal sinuses of bovids (Fig. 1C–E) are air-filled spaces that originate from the nasal cavity, located wholly within the vaulted (expanded) frontal bone. The sinuses are sandwiched between two layers of cortical bone: one at the outer table of the skull (hereafter referred to as the 'external cortex') and one forming part of the surface of the endocranial cavity ('internal cortex') – and may extend into the horncores. Bony struts (usually numbering between four and six on each side in goats, with a typical thickness of 1 mm or less) may divide the sinuses into a series of interconnected chambers. The idea of frontal sinuses as 'shock absorbers' is often repeated in the literature (e.g. Geist, 1966; Schaffer and Reed, 1972) and has even been used, by analogy, to reveal the function of sinuses in extinct dinosaurs such as *Triceratops* (Molnar, 1977; Forster, 1996). Despite this, the idea of sinuses as protective structures remains completely untested.

Certainly, it is not the empty space of a sinus that absorbs shocks. As suggested by Schaffer and Reed (Schaffer and Reed, 1972), the outer walls of the sinus or the struts within the sinus could deform during impact, in place of deformation of the endocranium. Thin walls of bone would be more deformable than solid bone. A related possibility is that the walls direct the forces away from biologically sensitive structures and towards sutures, where further deformation takes place.

Any discussion of sinus function must also consider the broadly accepted idea of the sinuses as a by-product of bony remodeling (e.g. Weidenreich, 1941; Edinger, 1950; Witmer, 1997). This mechanism follows models of bone adaptation discussed by Roux (Roux, 1881) and others, in which the

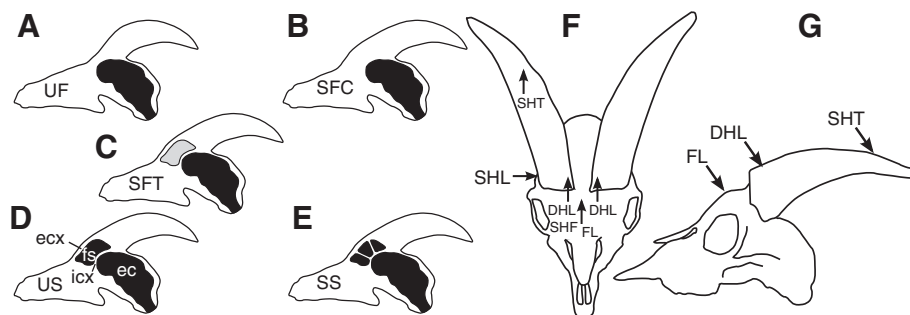


Fig. 1. Schematics of models and loading conditions used in this study. (A–E) Schematics of hypothetical goat skulls in parasagittal section. (A) Unvaulted frontal (UF); (B) vaulted cortical bone-filled frontal (SFC); (C) vaulted trabecular bone-filled frontal (SFT); (D) vaulted frontal with unstrutted sinus (US); (E) vaulted frontal with strutted sinus (SS). The endocranial cavity (ec) and sinuses (fs) are indicated in black and trabecular bone is indicated in gray, along with the external cortex (ecx) and internal cortex (icx) of the frontal bone. Schematics of finite element models in (F) dorsal and (G) left lateral views, with arrows indicating the location and direction of modeled loads for various loading cases. DHL, double horn loading case; FL, frontal loading case; SHF, single horn front loading case; SHL, single horn lateral loading case; SHT, single horn tip loading case.

unpneumatized skull contains areas of bone that are not necessary for mechanical support. Osteoclasts associated with pneumatic diverticula from the nasal cavity remove the structurally unnecessary bone, producing a sinus within a more ‘optimized’ skull (Witmer, 1997). Under this hypothesis, the frontal bone that contains the sinus, and not the sinus itself, is the more important structure. The frontal bone could have its current morphology for any number of reasons, such as structural support of the horns, but the shape of the sinus itself reflects only the loads placed upon the skull (Preuschoft et al., 2002). Importantly, this concept is not mutually exclusive of other functions for the sinuses or the vaulted frontal bone, such as shock absorption.

The idea of sinuses as somehow producing ‘optimal’ structures (greatest strength with least materials) remains extraordinarily difficult to test with conventional experimental methods. A similar problem plagues the shock absorption hypothesis. Thus, finite element modeling (FEM) was used in this study to test the effects of cranial sinuses in the domesticated goat *Capra hircus*.

Hypotheses

Finite element models of variable morphology – including skulls with strutted sinuses, unstrutted sinuses, sinuses filled with trabecular or cortical bone, and skulls completely lacking sinuses and a vaulted frontal bone (Fig. 1A–E) – were constructed in order to test three (not mutually exclusive) hypotheses:

(1) Sinuses function as shock absorbers (Schaffer and Reed, 1972). Strain energy, used here as a proxy for shock absorption in static analysis (see Materials and Methods), should be elevated in the frontal bones for skulls with sinuses relative to skulls without, reflecting the fact that this energy then would not be transferred into the endocranial cavity. A second aspect of shock absorption could be effected by sinuses directing the strain that results from forces placed on the horns away from the endocranial cavity (Schaffer and Reed, 1972). A skull with sinuses that is otherwise identical in shape to a skull that lacks sinuses (compare Fig. 1E with Fig. 1B) should experience higher strains within the endocranial cavity, simply because the removal of bone reduces the overall stiffness of the frontal bones and results in greater overall deformation. But if the removal of bone to form a sinus results in a structure that directs the force of impact away from the endocranial cavity (or towards different regions), the skull with sinuses still should experience lower strains within the bone surrounding the endocranial cavity, as well as exhibit a different spatial pattern of

strain distribution. The struts within the sinus may also play a role in this regard, with similar predictions.

(2) The dorsally vaulted and thickened frontal bone, not the sinus, is important for protecting the brain. If this is true, it was expected that a skull without the normal vaulted frontal bone (Fig. 1A) would experience significantly higher stress, strain, deformation and strain energy in the endocranial cortex or frontal bone than skulls with either a solid vaulted frontal bone or a vaulted frontal with sinuses (Fig. 1B–E).

(3) Frontal sinuses improve ‘structural efficiency’ (i.e. reduce the amount of unloaded bone) for skulls with vaulted frontal bones. This hypothesis was tested by comparing histograms of stress distribution within the frontal bones for models with solid and hollow frontals. It has been predicted that a skull with a completely solid frontal would have a significant population of unloaded bone segments in the area where the sinus would otherwise be located (using von Mises stress, a scalar approximation of total stress calculated from all of the principal stress vectors, as a proxy for loading). Sinuses thus optimize the skull by removing unloaded bone.

MATERIALS AND METHODS

The domesticated goat (*Capra hircus* Linnaeus 1758) was chosen for this study because of the availability of experimental data on cranial impact for validation of the FE models (Jaslow and Biewener, 1995) (see Appendix 1). Model geometry was based on CT scans of the skull of a young male goat, with an in-plane pixel resolution of 0.49 by 0.49 mm and interslice spacing of 2.5 mm. Visual inspection of renderings of the data indicated that this slice spacing adequately portrayed the cranial structures of interest in this study. The CT slices were imported into the modeling package SolidWorks 2003 (SolidWorks Corp., Concord, MA, USA), in which bone and keratinous horn sheath were traced manually on each slice, and the tracings were lofted into a three-dimensional solid model (Fig. 2A). In order to simplify the geometry of the model, the foramina of the basicranium (except for the foramen magnum) and the paroccipital and styloid processes were not incorporated into the model. Because the primary area of interest in the model was the cranial roof and not the cranial base, these simplifications were considered appropriate.

Numerous studies demonstrate that sutures exhibit elevated strain magnitudes relative to the surrounding bones and thus affect strain distribution across the skull (e.g. Behrens et al., 1978; Herring and

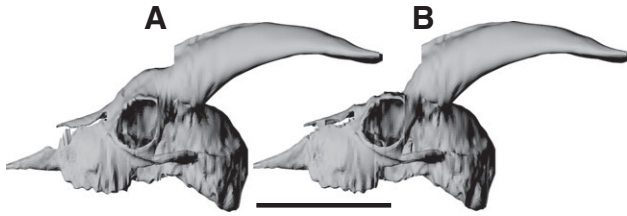


Fig. 2. Left lateral views of finite element meshes for (A) the models with vaulted frontals (including the models with strutted and unstrutted sinuses and solid frontals) and (B) the model with unvaulted frontals. Scale bar, 10 cm.

Teng, 2000; Jaslow, 1990). Jaslow and Biewener (Jaslow and Biewener, 1995) even suggested that the sutures play a major role in shock absorption in goats. Thus, the models were constructed with lines of compliant elements for the interfrontal and frontoparietal sutures. These sutures are closest to the sinuses (the area of interest) and the horncores (the area of primary loading) and thus are most likely to affect the results. Importantly, the sutures themselves were not modeled here, but rather a sutural zone that included both the suture and surrounding bone. For this reason, it was not appropriate to give the suture zones material properties for sutures that are reported in the literature (e.g. Radhakrishnan and Mao, 2004). Instead, the suture zones were given properties intermediate between cortical bone and sutural material [elastic modulus (E)=0.400 GPa, Poisson's ratio (ν)=0.28, density (ρ)=1.13 g cm⁻³], reflecting the composite nature of the suture zone. These properties were determined by iteration of a test model, until it displayed strains across the sutures similar to those reported by Jaslow and Biewener (Jaslow and Biewener, 1995) for their *in vitro* experiments on goat heads.

Four model geometries were constructed in order to test the functional effects of different morphologies of the frontal (Figs 1 and 2). The first model ('unvaulted frontal') lacked sinuses, and the contour of the frontal was smoothed to a thickness approximately equal to that of the combined inner and outer tables of bone in the unmodified skull (Fig. 1A). The resulting geometry was reminiscent of some bovids that lack enlarged frontal sinuses, such as members of the genus *Gazella*. The second model consisted of a skull completely lacking the frontal sinuses; the space within the vaulted frontal normally occupied by the sinuses was filled with bone (Fig. 1B,C). Two variants of this model were considered in the analysis, by setting the material properties of the bone occupying the location of the sinus to that of cortical bone ('vaulted cortical bone-filled frontal') or trabecular bone ('vaulted trabecular bone-filled frontal'; see below). The third model ('unstrutted sinus') comprised a skull with a simple unstrutted sinus cavity (Fig. 1D). Here, the boundaries of the frontal sinuses were simplified to eliminate all struts within the sinus, except for the midline strut at the interfrontal suture. The final model incorporated a complex frontal sinus, with all struts included (Fig. 1E). This model ('strutted sinus') represented the original goat skull. All models were otherwise identical.

The model geometries were imported into the finite element modeling package ALGOR FEMPro (v.20.0; Algor, Pittsburgh, PA, USA). Within FEMPro, the model was meshed using mixed brick elements. Mesh density was set to allow for multiple element thickness across the regions of experimental interest, such as the cranial vault, to achieve a more realistic solution. Owing to the size and complexity of the models, it was not feasible to conduct convergence tests with varying mesh densities. The model with an

unvaulted frontal had 152,750 nodes and 382,972 elements; the models with vaulted solid frontals had 134,709 nodes and 363,407 elements; the model with unstrutted sinuses had 119,748 nodes and 309,790 elements; and the model with strutted sinuses had 119,436 nodes and 311,503 elements.

All models used identical material properties. Because properties for goat cranial bone have not been published, it was assumed that values based on averages of measurements from primate cranial vaults were appropriate substitutes (E =14.550 GPa, ν =0.28, ρ =1.725 g cm⁻³) (Wang et al., 2006). Properties of trabecular bone within the frontals (for models with vaulted, trabecular bone-filled frontals) were based on published measurements from human tibiae (E =0.637 GPa, ν =0.28, ρ =0.2634 g cm⁻³) (Ashman et al., 1989). With the exception of Poisson's ratio, to which an arbitrary value of 0.30 was applied, properties for the horn sheath were adapted from those published for other bovids (E =3.900 GPa, ν =0.30, ρ =1.3 g cm⁻³) (Kitchener, 1991). Linear isotropic material properties were assumed, but cranial bone may have a high degree of anisotropy, potentially affecting analysis results (Strait et al., 2005). However, the present study is largely focused on patterns, not on precise values. Several studies have found that isotropic material properties, if appropriately selected, may be adequate for broadly characterizing most aspects of strain distribution within a skull (Metzger et al., 2005; Strait et al., 2005). Thus, anisotropic properties were not considered a major concern. For the same reasons, and because appropriate data are not available for goats, uniform material properties were used across the skull (except for the areas of trabecular or cortical bone within the frontal for certain models, keratin and sutures).

Static versus dynamic models

Shock absorption implies a dynamic component – deformation of a structure over time. Dynamic finite element analyses incorporating skull deceleration during impact are technically feasible, but require a set of data (duration of impact, motion of skull during impact, etc.) not currently available, as well as massive computing power for the resolution of models considered here. Strain energy, which is the potential energy stored within a deformed material (Hibbeler, 1997), presents a relevant proxy for examining shock absorption in static models. Briefly, an object under load deforms and converts the kinetic energy of impact into strain energy. This conversion reduces the accelerations acting on the skull. Strain energy stored in one region of a structure (the walls of the frontal bone and frontal sinuses) is not transferred elsewhere (e.g. as vibrations in the walls of the endocranial cavity).

Loading conditions

The skulls were modeled at the moment of peak force during impact, as estimated from values provided in previous studies (Jaslow and Biewener, 1995). Five loading cases of equal total magnitude (1088 N) were tested here, in order to examine the effects of different locations and directions of loading upon the skull (Fig. 1F,G). In the first loading case (double-horn loading), equal loads of 544 N were applied to the anterior surfaces of both horn sheaths at their proximal ends, for a total force of 1088 N. The forces were angled so that their combined vector passed through the center of the foramen magnum. Biologically, these loading conditions were considered to be a realistic representation of head-butting behavior in the goat (Jaslow and Biewener, 1995). Additionally, this loading condition was comparable with that used for *in vitro* experiments on goat crania by Jaslow and Biewener, allowing for comparison of the model with their data (Appendix 1). In the second loading

case (single horn front loading), a load of 1088 N was applied to the anterior surface of the base of the right horn sheath only (at the same angle as in the double-horn loading condition). In the third loading case (single horn lateral loading), a medially directed load of 1088 N was applied to the lateral surface of the base of the right horn sheath only. In the fourth loading case (single horn tip loading), a load of 1088 N was applied to the rostral surfaces of the right horn sheath approximately two-thirds of the way distally along its length. In the fifth and final loading case (frontal loading), a load of 1088 N was applied to the dorsal surface of the middle of the frontal bone, rostral to the base of the horncores. The angle relative to the base of the skull was identical to that used in double-horn loading; the only difference was in the location of the load relative to the base of the horn.

Constraints

The models were constrained at the occipital condyles from translation and rotation in all planes. This followed an assumption of several previous studies, that the occipital region is held relatively steady by the vertebrae and cervical musculature during impact (Schaffer and Reed, 1972). All models had identical constraints.

Comparison of results

Results were extracted for two areas: (1) the bony surface of the endocranial cavity; and (2) the frontal bone, excluding the surface of the endocranial cavity (Fig. 3). In order to evaluate hypotheses related to the role of the sinuses in protecting the brain and associated structures, values for principal strains were extracted for nodes of elements lining a region of the bony surface of the endocranial cavity. These nodes were located in the dorsal half of the cavity, exclusive of the region of the cribriform plate, rostral to the frontoparietal suture, and excluding values from the interfrontal suture (Fig. 3B). This region was selected because it was closest to the frontal sinuses (hence most likely to be affected by any changes in their morphology) and furthest from the occipital condyles (a region likely to have elevated values of stress and strain due to

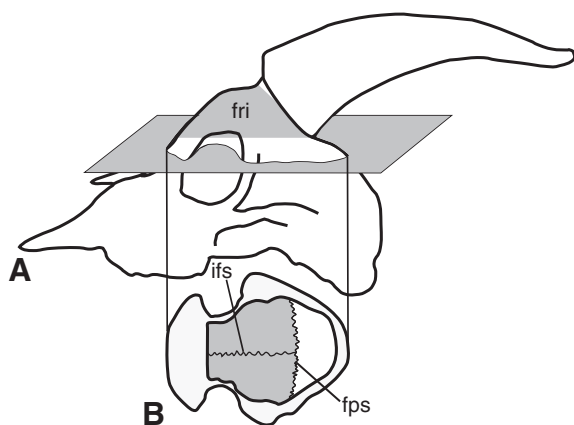


Fig. 3. Schematic indicating the location of nodes sampled for further analysis. (A) Schematic in left lateral view, with the location at which nodes were sampled within the frontal bone indicated by 'fri'. This view also indicates the location of the plane across which the endocranium was 'opened' in order to visualize principal strain patterns on the roof of the endocranial cavity. (B) View of the internal surface of the calvaria, with the dark gray area indicating the region of the endocranium that was sampled for the analyses presented in Tables 2 and 3 and Tables S2 and S3 in the supplementary material, and illustrated in Figs 4 and Fig. S1 in the supplementary material. fps, frontoparietal suture; ifs, interfrontal suture.

the constraints there). Graphical plots of strain were also generated, in order to visualize its distribution of across the surface of the endocranial cavity.

In order to evaluate hypotheses of how the sinuses affect the structural efficiency of the frontal, nodes were sampled from the entire frontal around and including the external cortex of the frontal sinus (exclusive of the free region of the horncores, the bony surface of the endocranial cavity and the sutures) (see Fig. 3A). Values for von Mises stress (giving an estimate of overall stress magnitudes in the model) and strain energy (indicating how much energy is stored by the frontal) were extracted for all of the nodes in this region, for each model.

Interpretation of results for the frontals was complicated. For example, it was expected *a priori* that average stress magnitudes should be greater throughout the model with sinuses than in the model with a solid vaulted frontal, because there was less bone to dissipate forces. The relative distribution of the stresses was considered to be more informative. Thus, histograms were used to visualize the distribution of nodal magnitudes for von Mises stress within the frontal, as has been commonly done elsewhere in the modeling literature (e.g. Van Rietbergen et al., 2003). Because the models differed in the numbers of elements in the frontal (reflecting whether the frontal was filled with bone or struts, or unvaulted), the nodal results were downsampled to 100,000 nodal values each (by random sampling without replacement) in order to create comparable histograms.

Strain energy was a bulk measure of total energy within the entire frontal bone, so no further corrections were necessary. The value was calculated as the sum of the strain energies of all of the elements of the region of the frontal bone outlined in Fig. 2 and Fig. 3A (the same region used for the analysis of von Mises stress). Models were loaded identically (the same force vector for each loading case, regardless of model morphology), so the value allowed a direct evaluation of which models stored the most energy from the applied load within the frontal.

The 50th (median) and 95th percentile values were calculated for each of the above samples (except for strain energy); mean and maximum values were not determined directly, because of the occurrence of rare extreme outliers. These extreme values occurred at sharp steps in the model geometry (an occasional byproduct of the process of generating the geometry from CT data in SolidWorks) or due to sharply shaped elements generated by the automated meshing routine. For example, for the model with strutted sinuses under the double-horn loading condition, the 95th percentile value for maximum principal strain within the body of the frontal bone was 858 N m^{-2} , whereas the maximum value was $24,454 \text{ N m}^{-2}$. Thus, the latter value is a modeling artifact that could exert extreme leverage on the mean. Instead, interquartile means (referred to hereafter as 'means', for simplicity) were calculated for all values between the 5th and 95th percentiles. All statistical calculations and histograms construction were completed in R (v.2.6, R Foundation for Statistical Computing, Vienna, Austria).

The models were validated by comparison to results from previously published *in vitro* experiments (Jaslow and Biewener, 1995). These comparisons are presented in Appendix 1.

RESULTS

Strain energy

The results presented here and in the following sections focus on the models under the double-horn (DHL) and frontal loading (FL) conditions, except where indicated. The DHL is highlighted

because it represents 'typical' results for a load to the horns, and the FL is useful as a point of contrast with the horn loading conditions because FL commonly occurs in bovids such as bison and musk ox. Under the double-horn loading condition (Table 1), the models with sinuses had the highest strain energy magnitudes within the frontal, followed by the model with unvaulted frontals (92% of the magnitude exhibited in the model with strutted sinuses), and models with vaulted bone-filled frontals (69% of the magnitude in the model with strutted sinuses, whether the frontal bone was filled with trabecular or cortical bone). Results were dramatically different for a load applied to the frontals. Here, the models with sinuses again had the greatest magnitudes of strain energy, but the model with vaulted trabecular bone-filled frontals ranked third (with 66% of the magnitude seen in the models with sinuses). The models with vaulted cortical bone-filled frontals (18% of the magnitude for models with sinuses) and unvaulted frontals (14% of the magnitude) had much lower values than did the other models.

Principal strains on the endocranial surface

For models with vaulted frontals under double-horn loading, the greatest magnitudes of principal strains (mean, median and 95th percentile values) were seen in the models with sinuses, followed by the models with trabecular bone-filled frontals and then cortical bone-filled frontals (Tables 2 and 3). The overall range of values

Table 1. Summary of strain energy values (in N m) in the frontal bone

Model	Load case	
	DHL	FL
UF	7870 (0.92)	6630 (0.14)
SFC	5974 (0.69)	9047 (0.18)
SFT	5898 (0.69)	32,387 (0.66)
US	8215 (0.96)	48,925 (1.00)
SS	8596 (1.00)	48,965 (1.00)

The number in parentheses indicates the ratio of magnitude to the magnitude for the model with strutted sinuses. All values are bulk values for the frontal bone.

Table 2. Summary of maximum principal strain values (in $\mu\epsilon$) in the dorsorostral region of the surface of the endocranial cavity (rostral to the fronto-parietal suture)

Load case	Percentile	Model geometry				
		UF	SFC	SFT	US	SS
DHL	50%	107	94	114	122	124
FL	50%	176	121	221	273	258
DHL	95%	354	272	297	313	310
FL	95%	516	251	356	453	434
DHL	Mean	135	112	133	144	148
FL	Mean	186	127	214	268	252

Table 3. Summary of minimum principal strain values (in $\mu\epsilon$) in the dorsorostral region of the surface of the endocranial cavity (rostral to the fronto-parietal suture)

Load case	Percentile	Model geometry				
		UF	SFC	SFT	US	SS
DHL	50%	-244	-180	-236	-249	-255
FL	50%	-191	-95	-208	-234	-241
DHL	95%	-568	-396	-453	-461	-492
FL	95%	-528	-342	-441	-453	-500
DHL	Mean	-279	-203	-256	-268	-279
FL	Mean	-242	-136	-233	-258	-259

across models typically spanned between 75 and 200 $\mu\epsilon$. The model with an unvaulted frontal varied in rank relative to the other models, but typically had magnitudes less than or approximately equal to the models with sinuses.

Under a load applied to the frontal, a similar ranking of magnitudes of principal strains occurred for models with vaulted frontals (Tables 2 and 3). Again, the model with an unvaulted frontal fell within the range exhibited for models with vaulted frontals (and had a smaller magnitude than the models with sinuses, except at the 95th percentile).

No major differences were found between models in the distribution patterns of strain across the bone lining the endocranial cavity (Fig. 4) under the double-horn loading condition. Sutural zones were under relatively high strain for both double-horn and frontal loading conditions. Under the frontal loading condition, the model with an unvaulted frontal was unique among the model geometries in the distribution of strain across the surface of the endocranial cavity (Fig. 4F,P). At the rostral end of the endocranial cavity, there was a zone of high principal strain magnitudes (Fig. 4F,P) (this was primarily a difference in spatial distribution rather than overall magnitude; Tables 2 and 3). This contrasted with the regions of lower strain immediately caudal to that zone. A very different pattern occurred in all four of the models with vaulted frontals, in which maximum principal strains were more evenly distributed across the surface of the endocranial cavity (Fig. 4G-J) and where greatest magnitudes of minimum principal strain were confined to the lateral edges of the region of interest (Fig. 4Q-T). The model with a cortical bone-filled frontal had consistently low magnitudes of strain across the endocranial region of interest for minimum principal strain, with a slight elevation of maximum principal strain at the caudal end (Fig. 4G,Q).

Von Mises stress in the frontal bone

Under the double-horn loading condition (Fig. 5A-E), the model with unvaulted frontals and the model with cortical bone-filled, vaulted frontals showed a greater concentration of low-magnitude values than seen in the models with sinuses (Fig. 5A,B,D,E). A peak of low-stress elements in the model with trabecular bone corresponded to elements with material properties

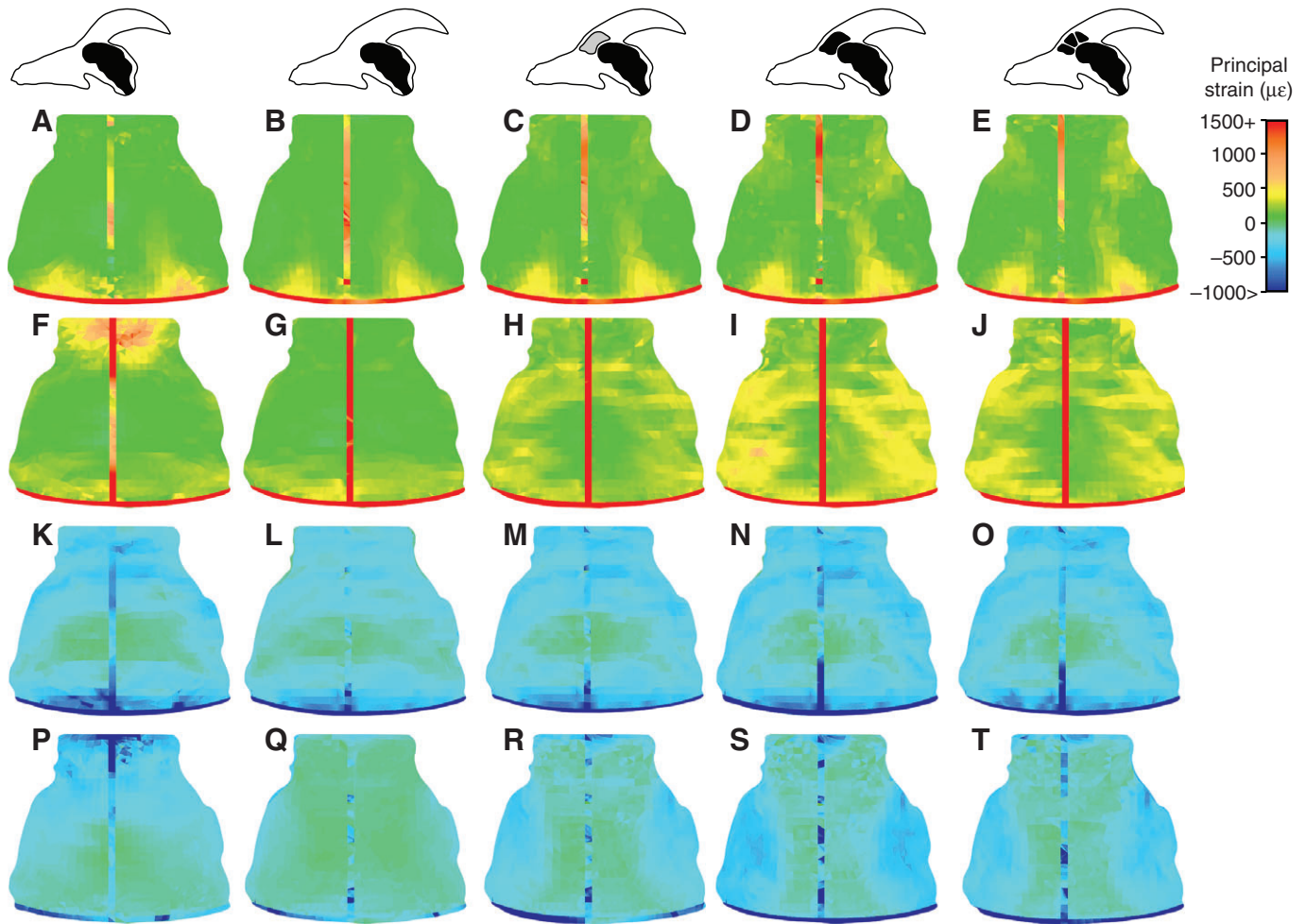


Fig. 4. View of the internal surface of the rostral region of the endocranial cavity, between the cribriform plate of the ethmoid (at the top of the images) and the frontoparietal sutures (at the bottom of the images), showing patterns of principal strains under the double-horn (A–E, K–O) and frontal (F–J, P–T) loading conditions. The top two rows (A–J) show maximum principal strain; the bottom two rows show minimum principal strain (K–T). From the left, the model geometries illustrated are unvaulted frontal (A, F, K, P), cortical bone-filled vaulted frontal (B, G, L, Q), trabecular bone-filled vaulted frontal (C, H, M, R), vaulted frontal with unstrutted sinus (D, I, N, S) and vaulted frontal with strutted sinus (E, J, O, T). The scale bar indicates principal strain magnitudes in microstrain ($\mu\epsilon$).

of trabecular bone (Fig. 5C). Under the frontal loading condition, the models with solid vaulted frontals and unvaulted frontals (Fig. 5F–H) all had prominent peaks of low stress elements in the frontal loading condition. Stress values were more evenly distributed in all models with sinuses (Fig. 5I, J).

Deformation

Overall deformation of the models was relatively consistent under loads applied to the horns. The bulk of the deformation occurred caudal to the base of the horncore, especially at the frontoparietal suture, regardless of frontal morphology (Movies 1 and 2 in the supplementary material). Most bony deformation occurred in the bone immediately rostral and immediately caudal to the suture, caused by the cranial vault warping outwards. Under the frontal loading condition, the models with vaulted frontals experienced little deformation of the endocranial cavity. Instead, the external cortex of the frontal exhibited the bulk of the deformation as the cortex was pushed inwards (Movie 3 in the supplementary material). Deformation in the model with the unvaulted frontal occurred as the bone at the front of the endocranial cavity was pushed inwards (Movie 4 in the supplementary material).

Results from other loading conditions

Results for additional loading conditions are summarized here. Ranks of strain energy magnitude for loads applied to a single horn (regardless of direction) broadly followed those seen in the model under the double-horn loading condition (see Table S1 in the supplementary material). Models with sinuses always had greatest magnitude, and the model with a vaulted cortical bone-filled frontal always had the least magnitude. The model with vaulted frontals had between 46 and 92% of the magnitude of strain energy seen in the model with vaulted strutted sinuses. For principal strain magnitudes in the surface of the endocranial cavity or within the external frontal cortex, the rank order of maximum, minimum or median values differed slightly in some cases, but there were few exceptions to the general patterns described above (Tables S2 and S3 in the supplementary material). Generally, magnitudes of principal strain for the model with unvaulted frontals fell within the range seen for or occasionally slightly higher than (by no more than $120\mu\epsilon$, but typically much less) seen in models with vaulted frontals.

Contrasting with the double-horn loading condition, patterns of principal strain were not symmetrical across the endocranial cavity

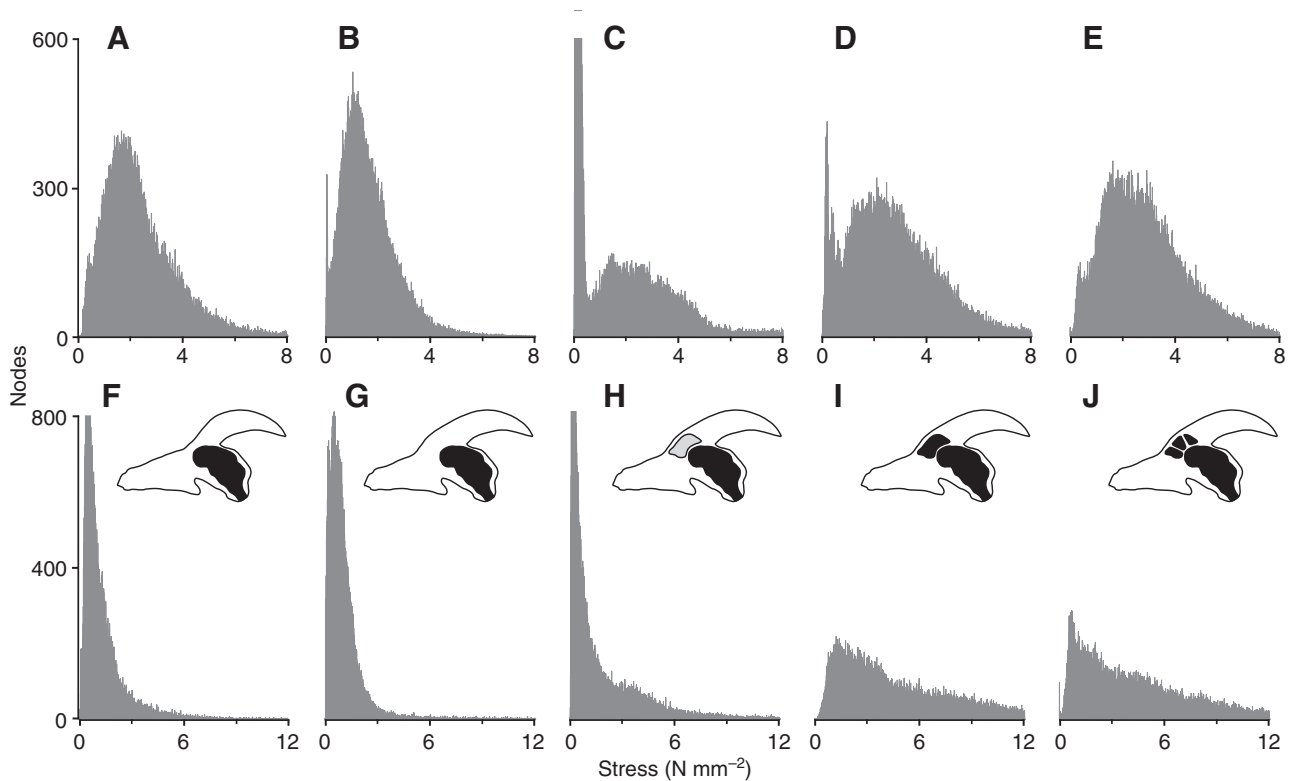


Fig. 5. Histograms of distributions of von Mises stress values within the frontal bone, exclusive of the surface of the endocranial cavity, for models under the double-horn loading (A–E) and the frontal loading (F–J) conditions. The vertical axis indicates the number of nodes with that value (all models normalized to 100,000 nodal values). For some parts (C,F,H), the peak has been truncated in order to conserve space. Model geometries illustrated include the unvaulted frontal (A,F), vaulted cortical bone-filled frontal (B,G), vaulted trabecular bone-filled frontal (C,H), vaulted frontal with unstrutted sinus (D,I) and vaulted frontal with strutted sinus (E,J).

when the load was applied only to a single horn (see Fig. S1 in the supplementary material). Strain magnitudes dropped greatly across the interfrontal suture in this case [consistent with the results of Jaslow and Biewener (Jaslow and Biewener, 1995)]. Patterns of distribution were quite similar across model geometries within each loading condition.

Just as in the frontal loading condition (and the double-horn loading condition, to a lesser extent), histograms of von Mises stress for the models with an unvaulted frontal and vaulted solid frontals showed prominent peaks of elements under low stress (Fig. S2 in the supplementary material).

DISCUSSION

Are sinuses shock absorbers?

As discussed previously, sinuses or a vaulted frontal could absorb shocks to the brain by two general mechanisms: (1) dissipating the energy of impact before it reaches the endocranial cavity; and (2) directing strain (and stress) away from the bone lining the endocranial cavity. Evidence supporting such a protective function was mixed.

If sinuses (or a vaulted frontal) have a major role in storing energy, models with these structures should show elevated strain energy in the frontal. Strain energy was always greatest for models with sinuses, appearing to support their suggested role in shock absorption. But a vaulted frontal alone did not always confer an advantage – under double-horn loading in particular, models with solid vaulted frontals stored a much lower proportion of the strain energy within the frontal than did the model with unvaulted frontals.

Thus, a sinus in combination with a vaulted frontal, rather than a vaulted frontal alone, was needed to maximize the shock absorption potential of the frontal bone.

Additionally, sinuses did not reduce strains on the surface of the endocranial cavity during most loads applied to the horns relative to a model with unvaulted frontals. In nearly all cases of horn loading, the model with frontals filled with cortical bone had the lowest overall magnitudes of strains (as measured by the median values), and the model with strutted sinuses (similar in morphology to real goat skulls) had the highest magnitudes (Tables 2 and 3; Tables S2 and S3 in the supplementary material). Most importantly, the overall patterns of strain distribution across the bone lining the surface of the endocranial cavity were quite similar across most models (Fig. 4; Fig. S1 in the supplementary material) (exceptions detailed below).

The model with trabecular bone-filled frontals generally behaved quite similarly to the models with sinuses (either strutted or unstrutted), when comparing the distribution of strains across the endocranial cavity. This was expected, in light of the fact that the elastic modulus for trabecular bone is much lower than that for cortical bone.

The frontal loading case was the only situation in which sinuses or a vaulted frontal seemed to have a major beneficial effect on strains on the surface of the endocranial cavity or strain energy within the frontal bone, over the model with unvaulted frontals. Models with sinuses or a vaulted frontal distributed the load more evenly across the endocranial bone for loads to the frontal. The advantages of this are clear: by distributing deformation across a wide area, the

risk of damage to dural sinuses or meningeal arteries (relatively delicate structures carrying blood to and from the brain) is minimized. Strains were highly concentrated at the rostral end of the endocranial cavity (beneath the point of load application) in the model with unvaulted frontals, and strain energy magnitudes were also much lower than for models with vaulted frontals (except for the model with a vaulted, cortical bone-filled frontal). Yet, frontal loading does not appear to be a particularly realistic loading condition for goats. Extensive behavioral observations on wild ibex (*Capra pyrenaica*, congeneric with the *Capra hircus* modeled here and also sharing its general frontal morphology) do not report any instances of blows applied to the frontals (Alvarez, 1990). Thus, the biological relevance of this loading condition is questionable for goats (although certainly important for animals with extensive frontal sinuses that do butt frontals, such as *Bison*).

In summary, sinuses (or more specifically, the bone surrounding the space of the sinuses) appeared at first glance to have shock-absorbing potential under most loading conditions. This may be due to the fact that the thin walls of the sinus deform slightly during impact, creating a sort of ‘crumple zone’, and morphologies without this thin wall (or a thin wall of cortical bone against a relatively deformable layer of trabecular bone) do not allow such deformation. Yet, magnitudes of strain energy within the model with unvaulted frontals often approached magnitudes seen in models with sinuses, and patterns of principal strains also conflict with the idea of sinuses as shock absorbers.

The extra bone associated with sinuses or vaulted frontals seemingly would offer significant benefits for strain reduction. Why, then, do these structures fail to offer much greater shock absorption than seen in unvaulted frontals or a greater strain reduction in the walls of the endocranial cavity, especially when compared to dramatically different skull morphologies with unvaulted frontals? The most likely explanation is that the vaulted frontal and its sinuses are poorly placed to offer much protection from the typical dorsoventral and rostrocaudal loads applied to the horns in life. Thus, the loads are directed away from the thickest part of the frontal, and directly into the thinner part of the braincase, where most of the deformation occurs. A biomechanically ‘better’ design (at least in light of desired endocranial strains and deformation) would place the horns atop or in front of the vaulted frontal, instead of at the rear of this structure. Instead, the caudal placement of the horns in goats and many other bovids, along with reorientation of the basicranium and other structures, may serve to reduce torque about the foramen magnum during head-butting (Schaffer and Reed, 1972; Jaslow, 1987). The morphology of the goat skull is clearly a trade off between multiple structural considerations.

The role of struts

In goats, the struts within the sinuses did not appear to have a major role in absorbing shocks or distributing loads applied to the frontals. In comparing the model with strutted sinuses to the model with unstrutted sinuses, very few differences were evident. The histogram distributions were virtually identical in most cases (Fig. 5; Fig. S2 in the supplementary material). Similarly, there were no appreciable or consistent differences between the two models when considering patterns of endocranial strains (Fig. 4; Fig. S1 in the supplementary material), or when considering strain energy within the frontal itself (Table 1; Table S1 in the supplementary material).

Do the struts have any function, then? One possibility is that the struts are just a by-product of sinus formation – bone that was ‘accidentally’ left behind by osteoclasts. The midline strut separating the right and left frontal sinus (a structure that was included in all

models) may be retained due to interactions between sutures (the interfrontal suture, in this case) and pneumatic epithelia (Farke, 2007). Another possibility is that the struts improve the overall strength of the frontal. However, given the extremely thin nature of some of these struts in *Capra*, this hypothesis appears doubtful. Additionally, many other bovids (e.g. *Alcelaphus* and *Damaliscus*) have sinuses with very few struts (Farke, 2007), with apparently little consequence. By contrast, bighorn sheep (*Ovis canadensis*) and Cape buffalo (*Syncerus caffer*) are notable for extensive strutting within their frontal sinuses [hundreds of struts, far beyond that seen in *Capra* (Schaffer and Reed, 1972); A.A.F., unpublished]. These species, and many of their close relatives, engage in extremely vigorous head-butting. It is quite possible that the numerous struts of such taxa do play a role in structural support and shock absorption, whereas struts are less important in goats. Comparative quantitative analyses of sinus morphologies are necessary in order to determine whether there is a correlation between the number of struts and behavior. Further finite element modeling may also prove useful.

Sinuses and ‘structural efficiency’

Areas of bone that experience only low magnitude stresses are not used in load transmission or shock absorption, so such regions could be thought of as unnecessary for the structural support of the skull. Thus, an efficient structure eliminates such elements. The histograms of von Mises stress produced for these models were consistent with this hypothesis (Fig. 5; Fig. S2 in the supplementary material). This was well-illustrated by models under the double-horn loading condition (Fig. 5B–E). The model with cortical bone-filled frontals had a relatively larger peak of low-magnitude stresses (and fewer high magnitude stresses) when compared with the models with sinuses or the model with trabecular bone-filled frontals. Replacing the cortical bone in the center of the frontal with trabecular bone or a sinus eliminated this peak of elements under low stress.

Why a vaulted frontal?

Although ‘structural efficiency’ and gains of shock absorption potential may explain the presence of a frontal sinus, it does little to explain why the frontal should be vaulted in the first place (when compared with other bovids, such as gazelles, that lack frontal vaulting). Certainly, in terms of strain energy, the vaulting does offer an advantage in shock absorption in some cases. Further study is needed to determine if this advantage is biologically meaningful or relevant over evolutionary time scales. A second possibility is that the vaulted frontal is needed as a base of support for the large horncores. The large base of support would increase the second moment of area, and hence strengthen the horns against applied loads. This is supported in part by the high proportion of frontal bone elements under low stress (Fig. 5A,F; Fig. S2A,F,K in the supplementary material) in skulls with unvaulted frontals. This indicates that a small proportion of elements is bearing a significant proportion of the load (especially considering that there is less bone volume when compared with any of the other skull morphologies). Alternatively, the enlarged frontals may increase the apparent ‘size’ of the skull (useful for visual display). A whole host of possibilities exist, many of which are untestable using the current techniques.

CONCLUSIONS

The finite element models developed in this study highlight the usefulness of this technique for testing the effects of varying cranial morphologies on cranial function. Significantly, the analyses presented are some of the first to change one aspect of the skull while leaving the rest of its morphology otherwise identical. Most

previous studies (e.g. Dumont et al., 2005; McHenry et al., 2006; Rayfield, 2005) have compared skulls of related animals with varying morphologies. Although a comparative taxonomic approach may also offer useful information (and be desirable for answering some questions), a clear interpretation of results may be muddled by disparate morphologies unrelated to the investigation at hand. Thus, digital manipulation of morphology is an often underutilized strength of finite element modeling for vertebrate skulls (e.g. Rayfield et al., 2007; Strait et al., 2007).

The present study finds mixed support for the frontal sinuses of the goat in protecting the skull against blows. Future work might investigate the shock-absorptive role of the keratinous sheaths of the horns; studies on attenuation of impact vibrations in horse hooves (e.g. Willeman et al., 1999) certainly warrant parallel investigations in goats. If the bone of the horncores is significantly less stiff than the bone of the cranial vault, the horncores themselves could play an important role in energy absorption during impact. Measurement of material properties within the goat skull would be important in this regard. Although vaulted frontals with sinuses offer shock absorbing potential under certain loading conditions, skulls with unvaulted frontals often show high shock absorption potential, too. Furthermore, frontal sinuses or even just a vaulted frontal bone do little to change the patterns of bone strain across the endocranium for most loading conditions. All of these supposed 'protective' structures are poorly placed for protecting the skull from most loads. Struts within the sinuses also seem to have little effect, at least for goats. Results are consistent, however, with the idea of sinuses removing 'unnecessary' bone from the frontal.

Several questions remain. If vaulted frontals and frontal sinuses are so poorly placed to deal with blows to the horns, why do so many head-butting taxa have such morphologies? Are sinuses more important in taxa (such as bison) that butt frontals directly? Are these morphologies indeed correlated with head butting? What other factors lead to enlargement of the frontal bone? The static models considered here present only one proxy for investigating the effects of head-butting on the brain. How is the brain tissue itself affected during the dynamic motions of head-butting? Further experiments, modeling and comparative anatomy may answer such questions.

APPENDIX 1 Validation methods

The finite element (FE) models were validated through comparison with the results of Jaslow and Biewener (Jaslow and Biewener, 1995). Their study placed strain gauges on bone at several points across goat heads under *in vitro* impact loads. Strain gauge locations from the experimental study that were comparable to the FE models included the anterior surface of the base of the

horncore, posterior surface of the base of the horncore, and the external aspects of frontal and parietal bones [fig. 1 of Jaslow and Biewener (Jaslow and Biewener, 1995)]. Due to inevitable differences in skull morphology and precise strain gauge placement as compared to the experimental results, strain gauge locations had to be approximated on the FE model. At each site of comparison, a set of nine nodes in a roughly rectangular pattern (three nodes in a triangular pattern for the posterior horncore, because of the limited exposed area) were selected for further analysis. Multiple nodes were sampled in order to mitigate the potential effects of any poor-quality elements.

Strain gauges only measure strain in two dimensions at most, so the three-dimensional strain vectors provided by FE models were not directly comparable. In order to measure the principal strains in the plane of the surface of the skull, the coordinate system was redefined separately for each area of the skull to coincide with the nodes sampled at each validation point. Then, the normal and shear strain tensors in the plane of the sampling region were extracted, and the magnitude and direction of planar maximum and minimum principal strains were calculated using standard engineering equations (Hibbeler, 1997).

Jaslow and Biewener (Jaslow and Biewener, 1995) published mean values and s.d. for each strain gauge site; modeled strains and strain orientations were considered realistic if they fell within two standard deviations of the experimental values. Ratios for maximum and minimum principal strain were also compared, as another measure of model performance. Results were validated in the model with strutted sinuses (reflecting real-life skull geometry) for the condition of double-horn loading.

Validation results

All principal strain magnitudes fell within two s.d. of experimentally determined values, and most fell within one standard deviation (see Table A1). This suggests that the finite element models produced a realistic picture of strain magnitudes relative to *in vitro* loading conditions, at least at the external surfaces of the frontal, parietal and horncores. Only two out of five sampled locations (on the left frontal and right parietal) produced angles of maximum principal strain within one s.d. of experimental values (and the rest were greater than two s.d. in difference). On a positive note, even the 'noncomparable' angles were within at least 26 deg. or less of the average of the experimental values. Ratios of maximum principal strain to minimum principal strain (reflecting the proportion of tensile strain to compressive strain) were quite similar across most locations. This indicated another broad level of similarity in the behavior of the computer model to *in vitro* experiments (regardless of differences in magnitude).

Table A1. Results of validation analysis

Location	Analysis	ϵ_1	s.d.	ϵ_2	s.d.	ϵ_1/ϵ_2	ϕ (deg.)	s.d.
Anterior horncore	FE model	344	**	-177	**	-1.94	-12	
Anterior horncore	<i>In vitro</i>	721	385	-379	253	-1.90	10	9
Posterior horncore	FE model	172	*	-668	*	-0.26	14	
Posterior horncore	<i>In vitro</i>	551	314	-1985	1171	-0.28	-12	10
Right frontal	FE model	130	*	-743	*	-0.17	-16	
Right frontal	<i>In vitro</i>	348	142	-1146	376	-0.30	4	10
Left frontal	FE model	147	*	-645	*	-0.23	9	**
Left frontal	<i>In vitro</i>	384	142	-1167	378	-0.33	7	7.5
Right parietal	FE model	9	*	-280	*	-0.03	21	**
Right parietal	<i>In vitro</i>	223	107	-772	306	-0.29	18	8.2

In vitro data are taken from Jaslow and Biewener (Jaslow and Biewener, 1995). *indicates that the FE model values are within 2 s.d. of the *in vitro* data; **indicates that model values are within 1 s.d. All strain (ϵ) values are given in microstrain ($\mu\epsilon$).

Differences between the experimental results and the finite element model may be due to subtle differences in shape or loading conditions between the model and experimental skulls. The material properties selected for the finite element model certainly affect results; strain magnitudes in the model were consistently lower than *in vitro*, suggesting that a less stiff elastic modulus would close the gap of strain magnitudes from two s.d. down to much less than one s.d. Application of anisotropic material properties could also bring the angles of principal strain closer to experimental observations.

LIST OF ABBREVIATIONS

DHL	double-horn loading case
<i>E</i>	modulus of elasticity
ec	endocranial cavity
ecx	external frontal cortex
fps	frontoparietal suture
fri	frontal region of interest
fs	frontal sinus
FE	finite element
FL	frontal loading case
icx	internal frontal cortex
ifs	interfrontal suture
SFC	model with vaulted, cortical-bone filled frontals
SFT	model with vaulted, trabecular-bone filled frontals
SHF	single horn front loading case
SHL	single horn lateral loading case
SHT	single horn tip loading case
SS	model with strutted sinuses
UF	model with unvaulted frontals
US	model with unstrutted sinuses
ρ	density
ν	Poisson's ratio
ϵ_1	maximum principal strain
ϵ_2	minimum principal strain
$\mu\epsilon$	microstrain

I thank my dissertation committee, including B. Demes, C. Forster, N. Kley, S. Judex and J. Rossie, for their helpful guidance throughout this research. Comments by two anonymous reviewers and A. Biewener further improved the manuscript. Discussions of FEM, pneumaticity and goat anatomy with D. Boyer, E. Dumont, A. Grossman, J. Hall, P. O'Connor, B. Patel, C. Ross, D. Strait, J. Tanner, L. Witmer and E. Yoo were invaluable. J. Shea provided the goat skull used for the models, and J. Georgi, J. Sipla, and the Department of Radiology at Stony Brook University Hospital assisted in acquiring the CT scan data. This work was supported by the Jurassic Foundation and a National Science Foundation Graduate Research Fellowship.

REFERENCES

- Alvarez, F. (1990). Horns and fighting in male Spanish ibex, *Capra pyrenaica*. *J. Mammal.* **71**, 608-616.
- Ashman, R. B., Rho, J. Y. and Turner, C. H. (1989). Anatomical variation of orthotropic elastic moduli of the proximal human tibia. *J. Biomech.* **22**, 895-900.
- Behrents, R. G., Carlson, D. S. and Abdelnour, T. (1978). *In vivo* analysis of bone strain about the sagittal suture in *Macaca mulatta* during masticatory movements. *J. Dent. Res.* **57**, 904-908.
- Dumont, E. R., Piccirillo, J. and Grosse, I. R. (2005). Finite-element analysis of biting behavior and bone stress in the facial skeletons of bats. *Anat. Rec.* **283A**, 319-330.
- Edinger, T. (1950). Frontal sinus evolution (particularly in the Equidae). *Bull. Mus. Comp. Zool. Harvard* **103**, 411-496.
- Farke, A. A. (2007). Morphology, constraints, and scaling of frontal sinuses in the hartebeest, *Alcelaphus buselaphus* (Mammalia: Artiodactyla, Bovidae). *J. Morphol.* **268**, 243-253.
- Forster, C. A. (1996). New information on the skull of *Triceratops*. *J. Vert. Paleontol.* **16**, 246-258.
- Geist, V. (1966). The evolutionary significance of mountain sheep horns. *Evolution* **20**, 558-566.
- Gurdjian, E. S. (1975). Re-evaluation of the biomechanics of blunt impact injury of the head. *Surg. Gynecol. Obstet.* **140**, 845-850.
- Herring, S. W. and Teng, S. (2000). Strain in the braincase and its sutures during function. *Am. J. Phys. Anthropol.* **112**, 575-593.
- Hibbeler, R. C. (1997). *Mechanics of Materials*. Upper Saddle River, NJ: Prentice Hall.
- Jaslow, C. R. (1987). A functional analysis of skull design in the Caprini. Ph.D. Thesis, University of Chicago, USA.
- Jaslow, C. R. (1990). Mechanical properties of cranial sutures. *J. Biomech.* **23**, 313-321.
- Jaslow, C. R. and Biewener, A. A. (1995). Strain patterns in the horncores, cranial bones and sutures of goats (*Capra hircus*) during impact loading. *J. Zool.* **235**, 193-210.
- Kitchner, A. C. (1987). Fracture toughness of horns and a reinterpretation of the horning behaviour of bovids. *J. Zool. (Lond.)* **213**, 621-639.
- Kitchner, A. C. (1988). An analysis of fighting of the blackbuck (*Antilope cervicapra*) and the bighorn sheep (*Ovis canadensis*) and the mechanical design of the horns of bovids. *J. Zool.* **214**, 1-20.
- Kitchner, A. C. (1991). The evolution and mechanical design of horns and antlers. In *Biomechanics in Evolution* (ed. J. M. V. Rayner and R. J. Wootton), pp. 229-253. Cambridge: Cambridge University Press.
- Levy, M. L., Olgur, B. M., Berry, C., Aryan, H. E. and Apuzzo, M. L. J. (2004). Birth and evolution of the football helmet. *Neurosurgery* **55**, 656-661.
- McDonald, J. N. (1981). *North American Bison: Their Classification and Evolution*. Berkeley: University of California Press.
- McHenry, C. R., Clausen, P. D., Daniel, W. J. T., Meers, M. B. and Pendharkar, A. (2006). Biomechanics of the rostrum in crocodylians: A comparative analysis using finite-element modeling. *Anat. Rec.* **288A**, 827-849.
- Metzger, K. A., Daniel, W. J. T. and Ross, C. F. (2005). Comparison of beam theory and finite-element analysis with *in vivo* bone strain data from the alligator cranium. *Anat. Rec.* **283A**, 331-348.
- Molnar, R. E. (1977). Analogies in the evolution of combat and display structures in ornithopods and ungulates. *Evol. Theory* **3**, 165-190.
- Preuschoft, H., Witte, H. and Witzel, W. (2002). Pneumatized spaces, sinuses and spongy bones in the skulls of primates. *Anthropol. Anz.* **60**, 67-79.
- Radhakrishnan, P. and Mao, J. J. (2004). Nanomechanical properties of facial sutures and sutural mineralization front. *J. Dent. Res.* **83**, 470-475.
- Rayfield, E. J. (2005). Aspects of comparative cranial mechanics in the theropod dinosaurs *Coelophysis*, *Allosaurus* and *Tyrannosaurus*. *Zool. J. Linn. Soc.* **144**, 309-316.
- Rayfield, E. J., Milner, A. C., Xuan, V. B. and Young, P. G. (2007). Functional morphology of spinosaur 'crocodile-mimic' dinosaurs. *J. Vert. Paleontol.* **27**, 892-901.
- Roux, W. (1881). *Der züchtende Kampf der Teile, oder die "Teilauslese" im Organismus (Theorie der funktionellen Anpassung)*. Leipzig: Wilhelm Engelmann.
- Schaffer, W. M. and Reed, C. A. (1972). The co-evolution of social behavior and cranial morphology in sheep and goats (Bovidae, Caprini). *Fieldiana* **61**, 1-88.
- Sinclair, A. R. E. (1977). *The African Buffalo: A Study of Resource Limitation of Populations*. Chicago: University of Chicago Press.
- Strait, D. S., Wang, Q., Dechow, P. C., Ross, C. F., Richmond, B. G., Spencer, M. A. and Patel, B. A. (2005). Modeling elastic properties in finite-element analysis: how much precision is needed to produce an accurate model? *Anat. Rec.* **283A**, 275-287.
- Strait, D. S., Richmond, B. G., Spencer, M. A., Ross, C. F., Dechow, P. C. and Wood, B. A. (2007). Masticatory biomechanics and its relevance to early hominid phylogeny: An examination of palatal thickness using finite-element analysis. *J. Hum. Evol.* **52**, 585-599.
- Van Rietbergen, B., Huiskes, R., Eckstein, F. and Rügsegger, P. (2003). Trabecular bone tissue strains in the healthy and osteoporotic human femur. *J. Bone Miner. Res.* **18**, 1781-1788.
- Wang, Q., Strait, D. S. and Dechow, P. C. (2006). A comparison of cortical elastic properties in the craniofacial skeletons of three primate species and its relevance to the study of human evolution. *J. Hum. Evol.* **51**, 375-382.
- Weidenreich, F. (1941). The brain and its role in the phylogenetic transformation of the human skull. *Proc. Am. Philos. Soc.* **31**, 320-442.
- Willemsen, M. A., Jacobs, M. W. and Schamhardt, H. C. (1999). *In vitro* transmission and attenuation of impact vibrations in the distal forelimb. *Equine Vet. J. Suppl.* **30**, 245-248.
- Witmer, L. M. (1997). The evolution of the antorbital cavity of archosaurs: a study in soft-tissue reconstruction in the fossil record with an analysis of the function of pneumaticity. *Soc. Vert. Paleontol. Mem.* **3**, 1-73.